Electronic Supplementary Material (ESI) for Nanoscale.

Theoretical Exploration of Quaternary Hexagonal MAB Phases and Two-Dimensional Derivatives

Yufang Yao, Nanxi Miao, Yutong Gong, Junjie Wang*,

State Key Laboratory of Solidification Processing, Northwestern Polytechnical University, Xi'an, Shaanxi 710072, People's Republic of China.

Supporting Figures

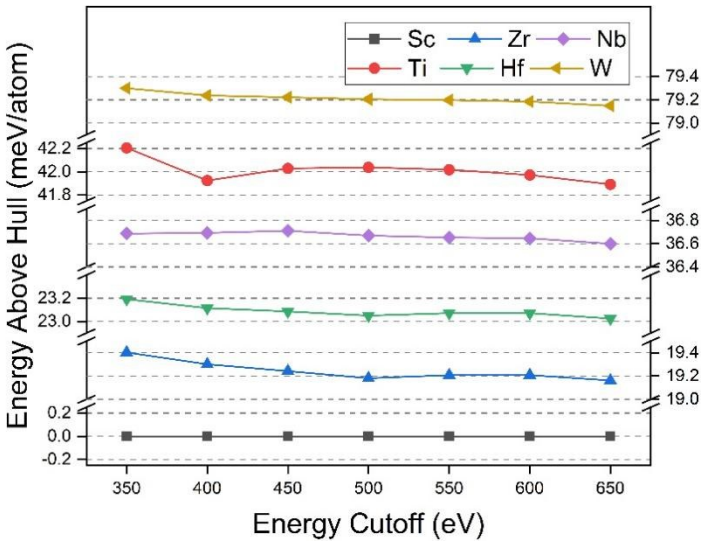

Figure S1. Convergence test of energy above convex hull of $(Mo_{2/3}M''_{1/3})GaB_2$ ($R\bar{3}m$) (where M'' = Sc, Ti, Zr, Hf, Nb, W) as function of energy cutoff.

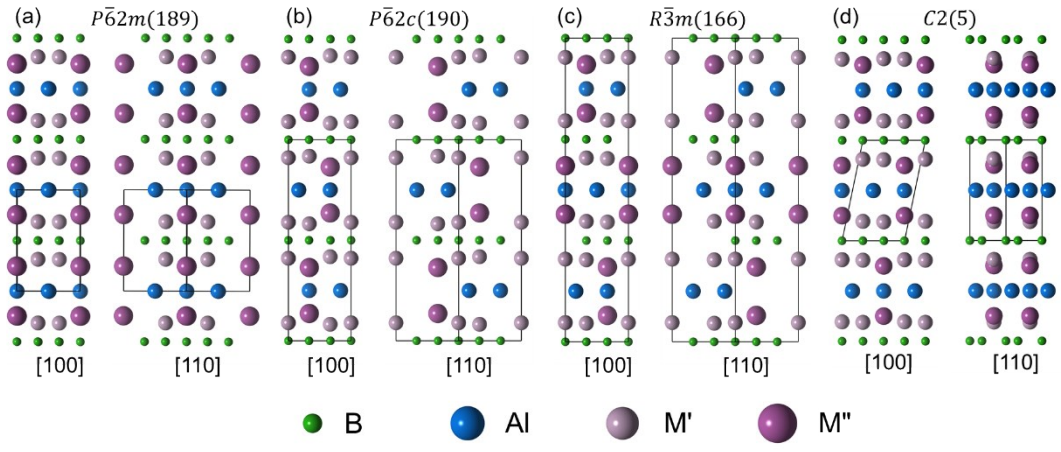

Figure S2. The crystal structure of predicted $(M'_{2/3}M''_{1/3})_2AlB_2$ quaternary *h*-MAB phases, (a) $P\bar{6}2m$ (189), (b) $P\bar{6}2c$ (190), (c) $R\bar{3}m$ (166) and (d) $C2$ (5).

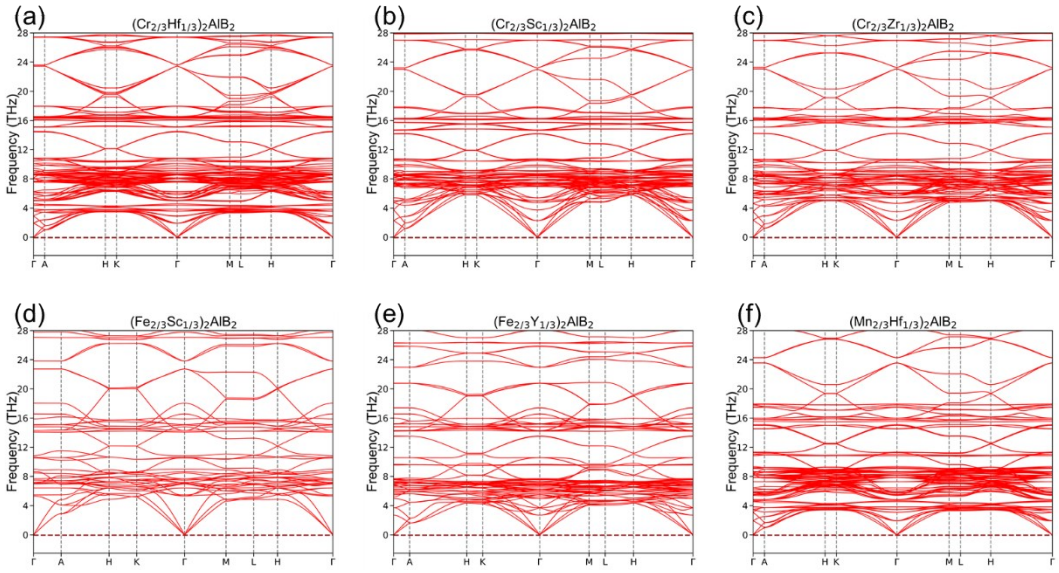

Figure S3. Phonon dispersion calculation for (a) $(Cr_{2/3}Sc_{1/3})_2AlB_2$, (b) $(Cr_{2/3}Zr_{1/3})_2AlB_2$, (c) $(Cr_{2/3}Hf_{1/3})_2AlB_2$, (d) $(Fe_{2/3}Sc_{1/3})_2AlB_2$, (e) $(Fe_{2/3}Y_{1/3})_2AlB_2$, (f) $(Mn_{2/3}Hf_{1/3})_2AlB_2$.

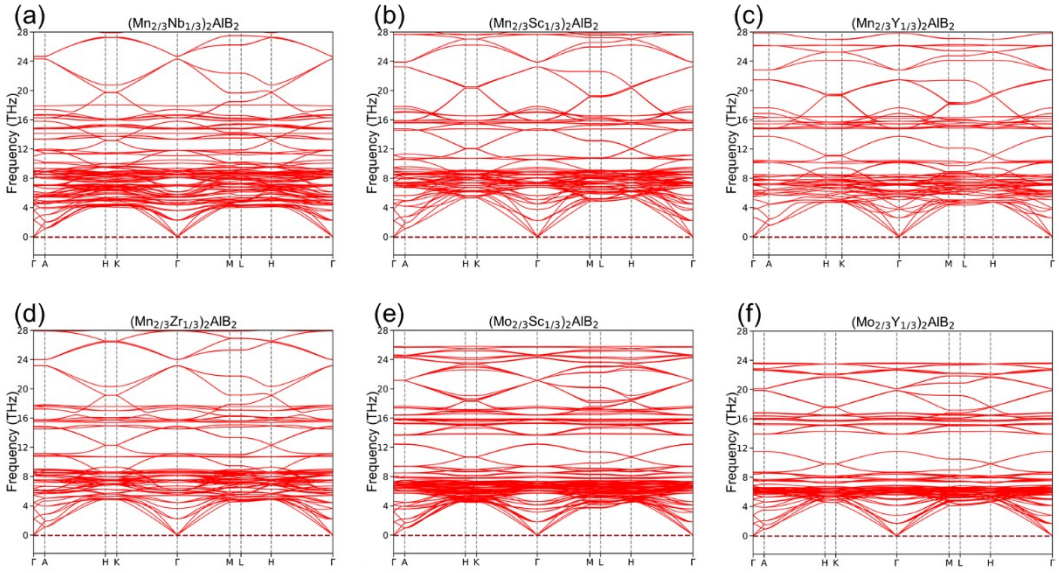

Figure S4. Phonon dispersion calculation for (a) $(Mn_{2/3}Nb_{1/3})_2AlB_2$, (b) $(Mn_{2/3}Sc_{1/3})_2AlB_2$, (c) $(Mn_{2/3}Y_{1/3})_2AlB_2$, (d) $(Mn_{2/3}Zr_{1/3})_2AlB_2$, (e) $(Mo_{2/3}Sc_{1/3})_2AlB_2$, (f) $(Mo_{2/3}Y_{1/3})_2AlB_2$.

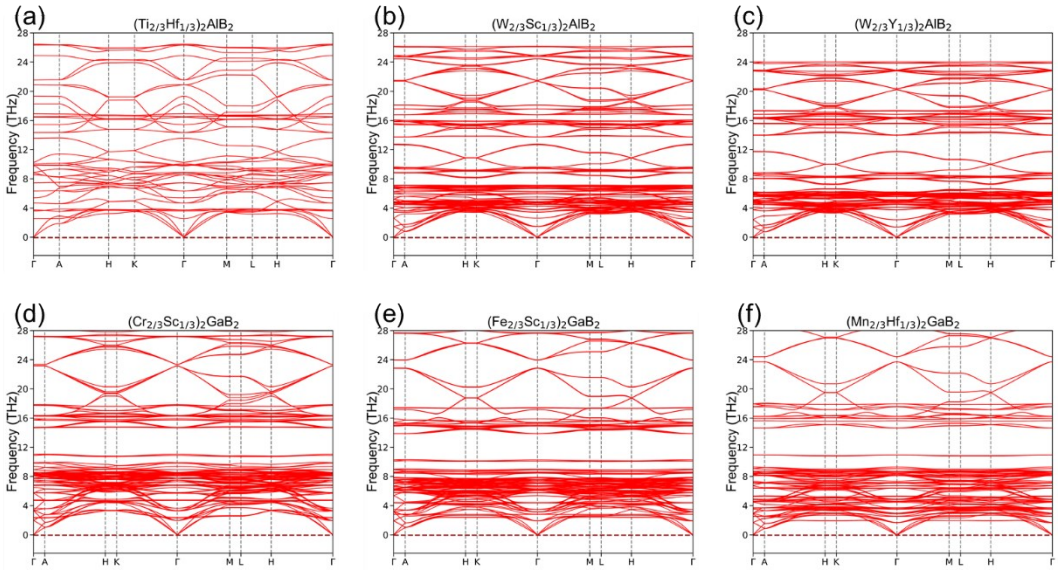

Figure S5. Phonon dispersion calculation for (a) $(Ti_{2/3}Hf_{1/3})_2AlB_2$, (b) $(W_{2/3}Sc_{1/3})_2AlB_2$, (c) $(W_{2/3}Y_{1/3})_2AlB_2$, (d) $(Cr_{2/3}Sc_{1/3})_2GaB_2$, (e)$(Fe_{2/3}Sc_{1/3})_2GaB_2$, (f)$(Mn_{2/3}Hf_{1/3})_2GaB_2$.

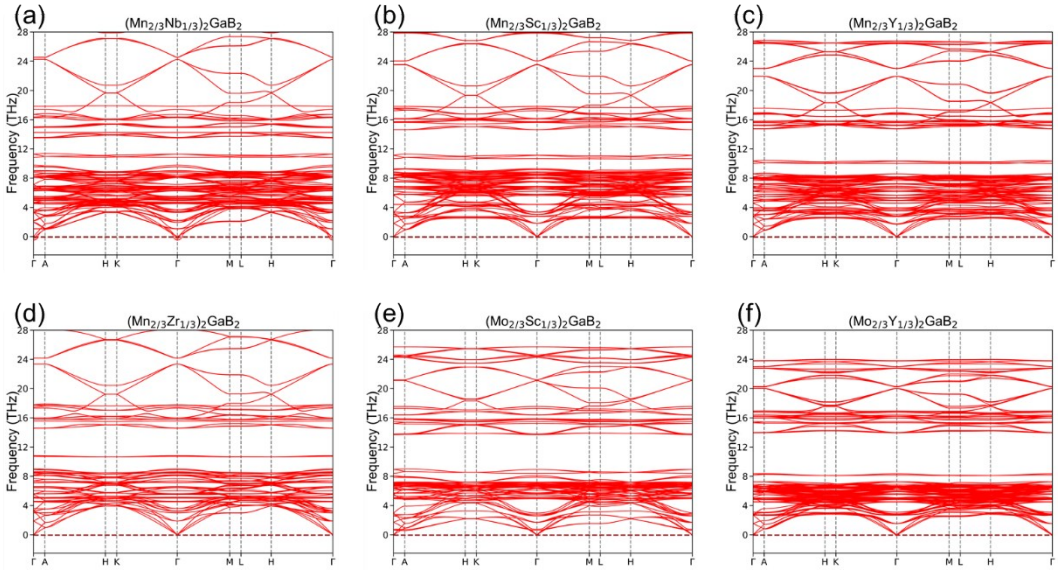

Figure S6. Phonon dispersion calculation for (a) $(Mo_{2/3}Nb_{1/3})_2GaB_2$, (b) $(Mn_{2/3}Sc_{1/3})_2GaB_2$, (c) $(Mn_{2/3}Y_{1/3})_2GaB_2$, (d) $(Mn_{2/3}Zr_{1/3})_2GaB_2$, (e)$(Mo_{2/3}Sc_{1/3})_2GaB_2$, (f)$(Mo_{2/3}Y_{1/3})_2GaB_2$.

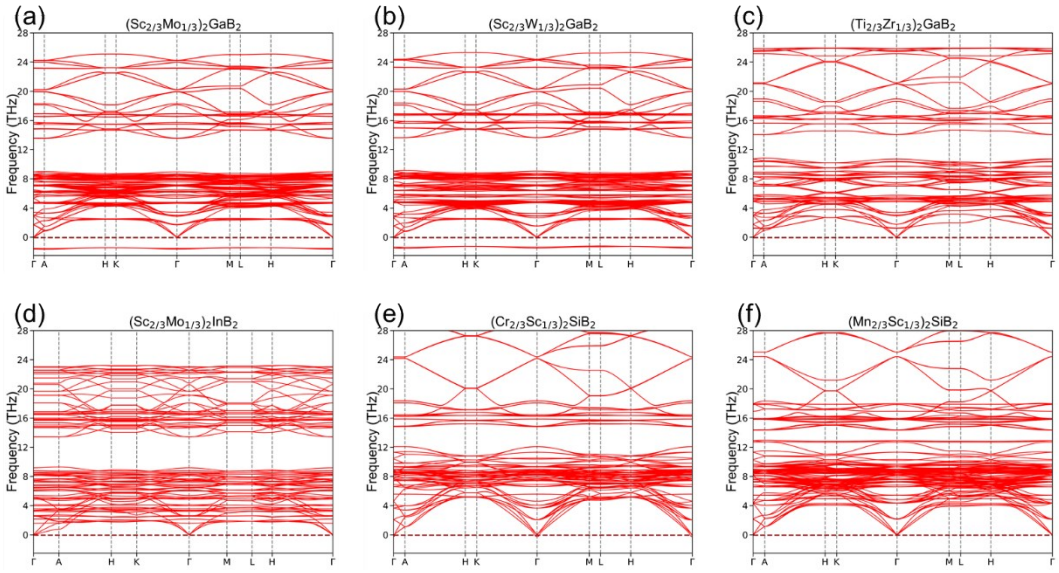

Figure S7. Phonon dispersion calculation for (a) $(Sc_{2/3}Mo_{1/3})_2GaB_2$, (b) $(Sc_{2/3}W_{1/3})_2GaB_2$, (c) $(Ti_{2/3}Zr_{1/3})_2GaB_2$, (d) $(Sc_{2/3}Mo_{1/3})_2InB_2$, (e)$(Cr_{2/3}Sc_{1/3})_2SiB_2$, (f)$(Mn_{2/3}Sc_{1/3})_2SiB_2$.

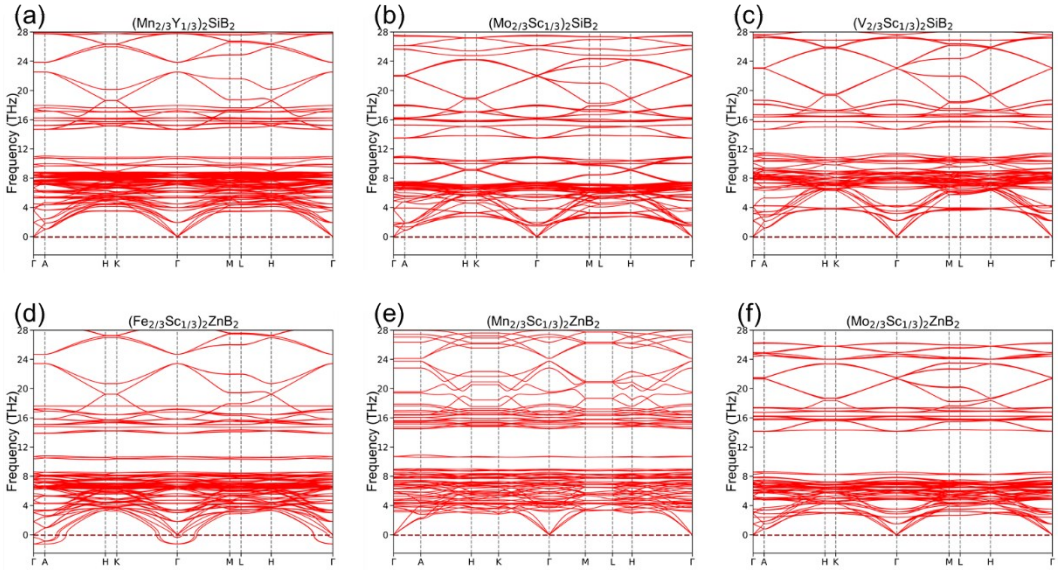

Figure S8. Phonon dispersion calculation for (a) $(Mn_{2/3}Y_{1/3})_2SiB_2$, (b) $(Mo_{2/3}Sc_{1/3})_2SiB_2$, (c) $(V_{2/3}Sc_{1/3})_2ZnB_2$, (d) $(Fe_{2/3}Sc_{1/3})_2ZnB_2$, (e)$(Mn_{2/3}Sc_{1/3})_2ZnB_2$, (f)$(Mo_{2/3}Sc_{1/3})_2SiB_2$.

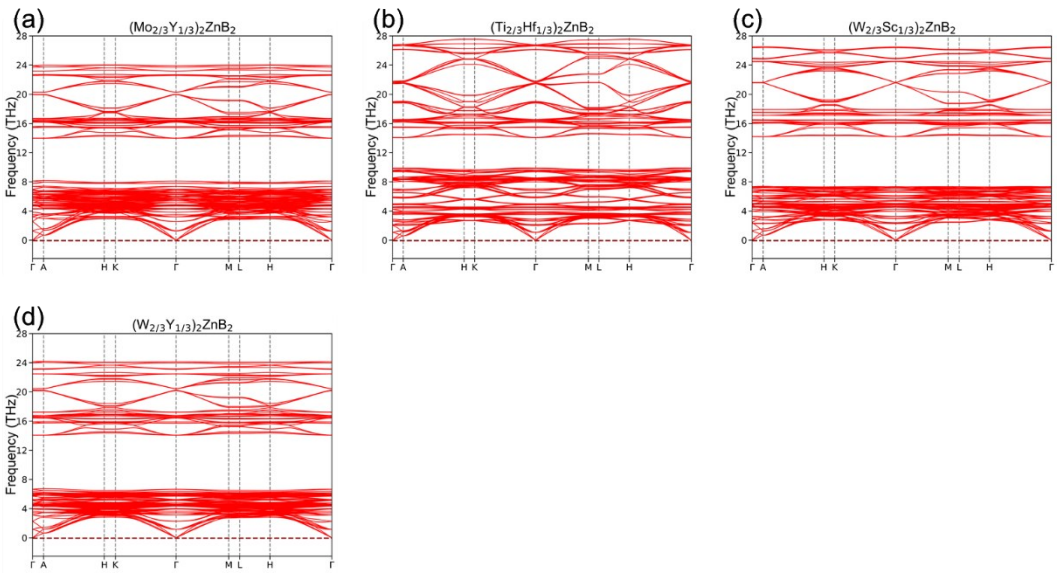

Figure S9. Phonon dispersion calculation for (a) $(Mo_{2/3}Y_{1/3})_2ZnB_2$, (b) $(Ti_{2/3}Hf_{1/3})_2ZnB_2$, (c) $(W_{2/3}Sc_{1/3})_2ZnB_2$, (d) $(W_{2/3}Y_{1/3})_2ZnB_2$.

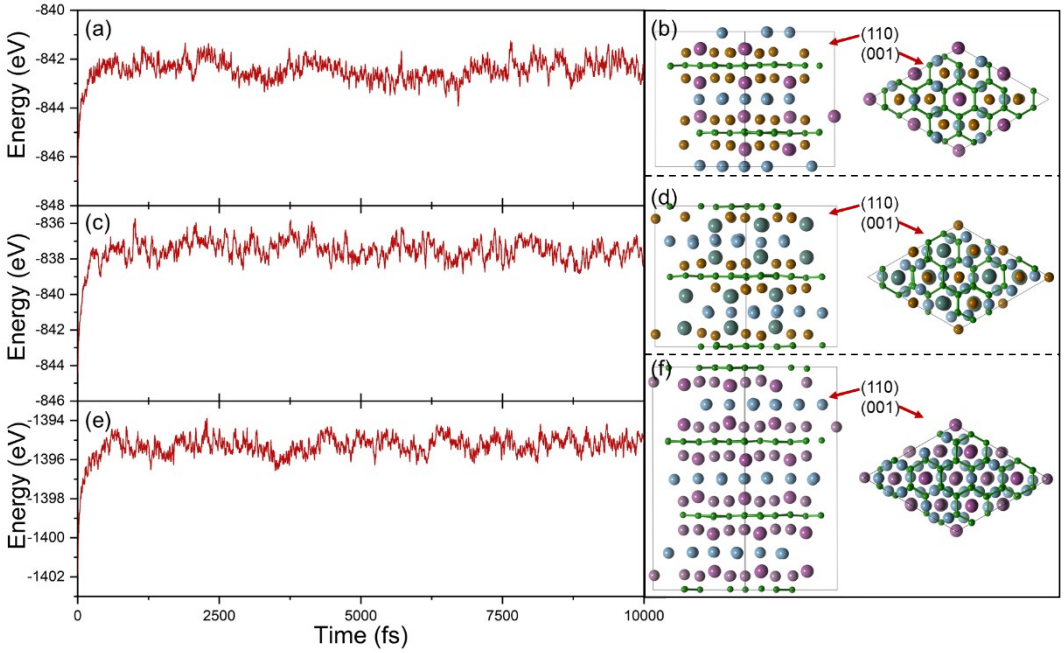

Figure S10. Ab initial molecular dynamics simulations at 300 K and equilibrium structures of three predicted quaternary *h*-MAB which represent three kinds of structures: (a) and (b) $(Fe_{2/3}Sc_{1/3})_2AlB_2$ ($P\bar{6}2m$); (c) and (d) $(Fe_{2/3}Y_{1/3})_2AlB_2$ ($P\bar{6}2c$); (e) and (f) $(Mo_{2/3}Sc_{1/3})_2AlB_2$ ($R\bar{3}m$).

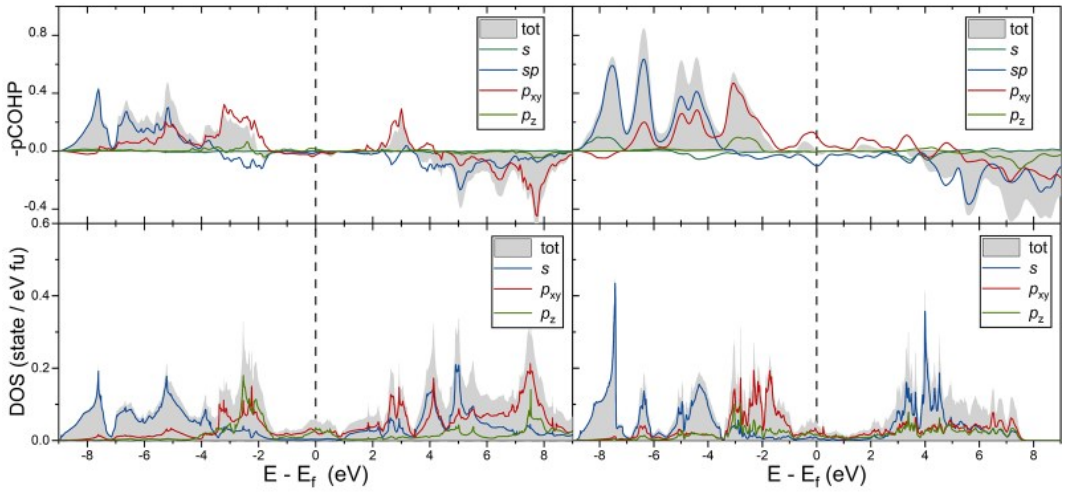

Figure S11. Calculated projected crystal orbital Hamilton population (pCOHP) for Al-Al in (a) Mo_2AlB_2 and (b) $(Mo_{2/3}Sc_{1/3})_2AlB_2$; Calculated projected density of states for element Al in (c) Mo_2AlB_2 and (d) $(Mo_{2/3}Sc_{1/3})_2AlB_2$.

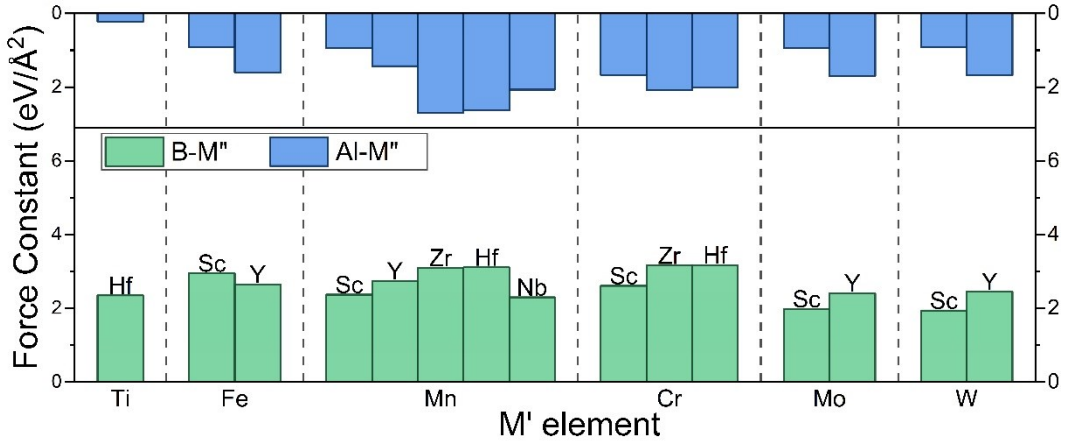

Figure S12. Comparison of calculated force constants for M"-Al and M"-B of the 15 predicted $(M'_{2/3}M"_{1/3})_2AlB_2$.

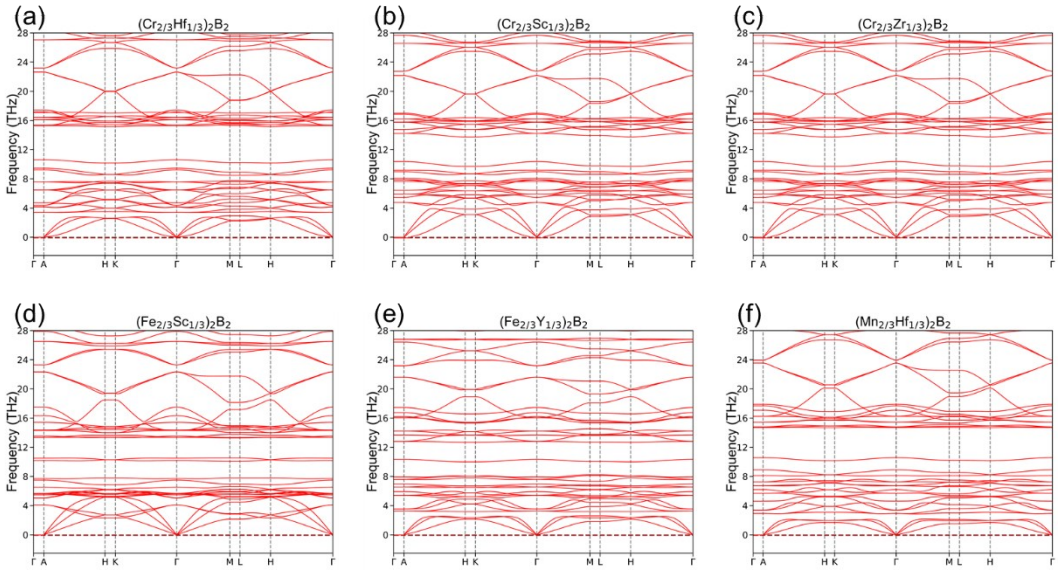

Figure S13. Phonon dispersion calculation for (a) $(Cr_{2/3}Hf_{1/3})_2B_2$, (b) $(Cr_{2/3}Sc_{1/3})_2B_2$, (c) $(Cr_{2/3}Zr_{1/3})_2B_2$, (d) $(Fe_{2/3}Sc_{1/3})_2B_2$, (e) $(Fe_{2/3}Y_{1/3})_2B_2$, (f) $(Mn_{2/3}Hf_{1/3})_2B_2$.

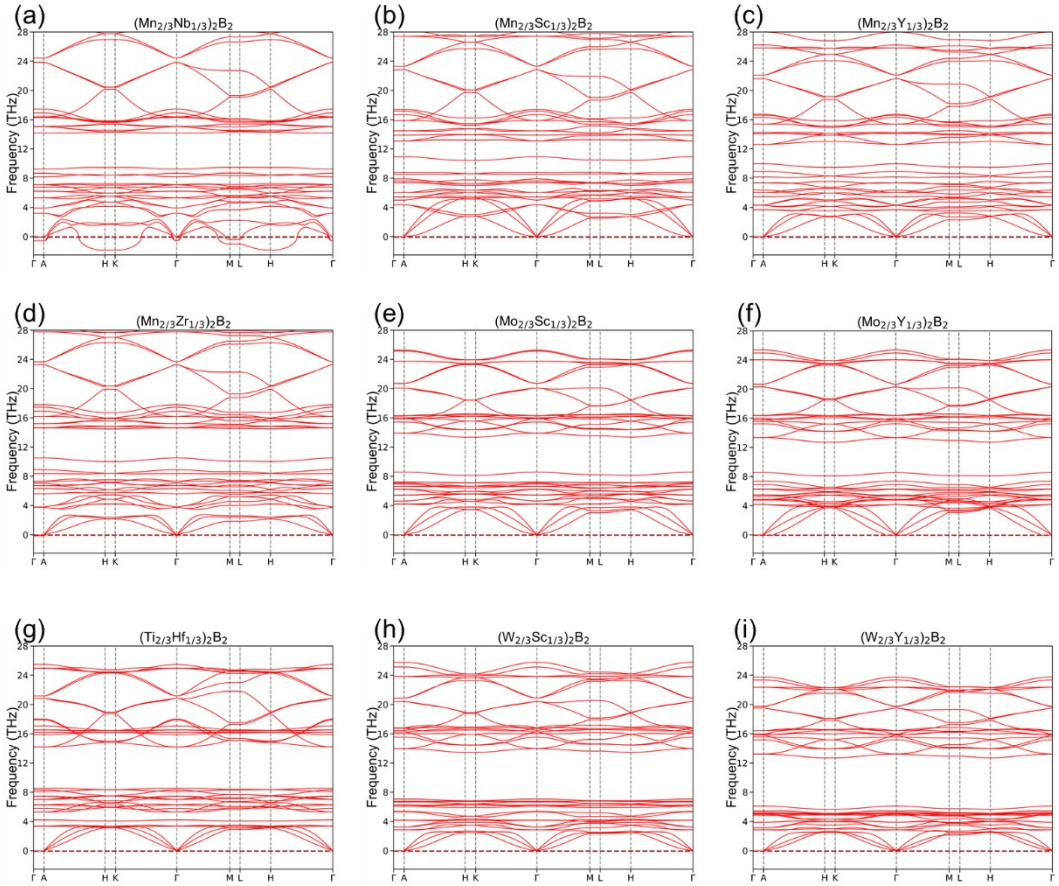

Figure S14. Phonon dispersion calculation for (a) $(Mn_{2/3}Nb_{1/3})_2B_2$, (b) $(Mn_{2/3}Sc_{1/3})_2B_2$, (c) $(Mn_{2/3}Y_{1/3})_2B_2$, (d) $(Mn_{2/3}Zr_{1/3})_2B_2$, (e) $(Mo_{2/3}Sc_{1/3})_2B_2$, (f) $(Mo_{2/3}Y_{1/3})_2B_2$, (g) $(Ti_{2/3}Hf_{1/3})_2B_2$, (h) $(W_{2/3}Sc_{1/3})_2B_2$, (i) $(W_{2/3}Y_{1/3})_2B_2$.

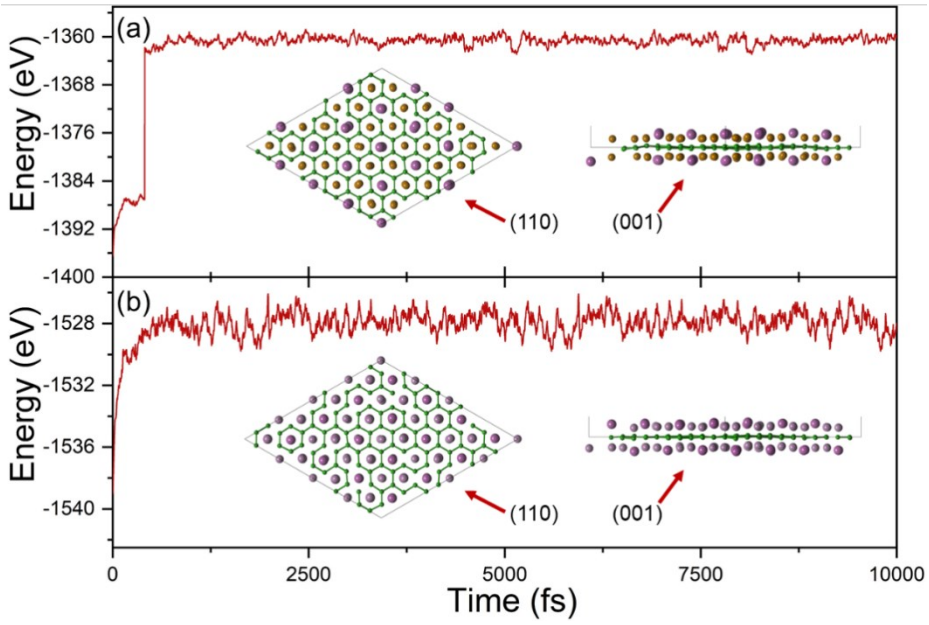

Figure S15. Ab initial molecular dynamics simulations at 300 K and equilibrium structures of two predicted quaternary *h*-MBenes which represent two kinds of structures: (a) $(Fe_{2/3}Sc_{1/3})_2B_2$ ($P6/mmm$); (b) $(Mo_{2/3}Sc_{1/3})_2B_2$ ($P\bar{3}m1$).

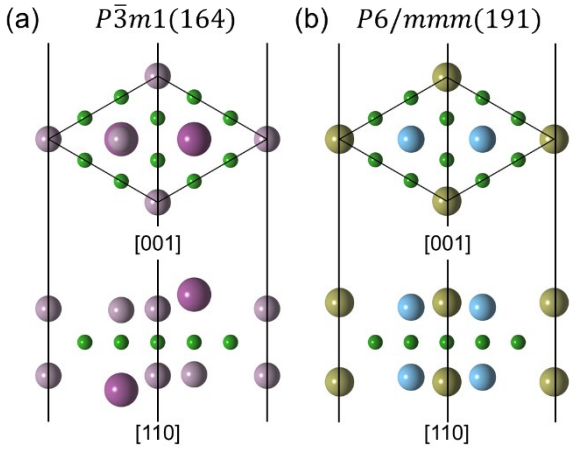

Figure S16. Top and side view of two kinds structure of *h*-MBenes: (a) $P\bar{3}m1(164)$; (b) $P6/mmm(191)$.

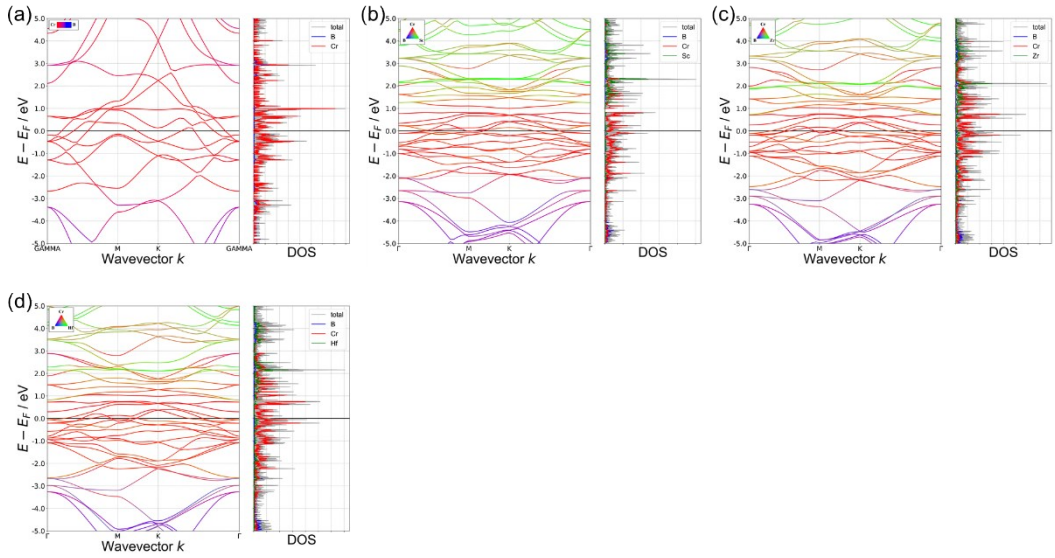

Figure S17. Calculated band structure and projected DOS for (a)Cr_2B_2, (b) $(Cr_{2/3}Sc_{1/3})_2B_2$, (c) $(Cr_{2/3}Zr_{1/3})_2B_2$, (d) $(Cr_{2/3}Hf_{1/3})_2B_2$.

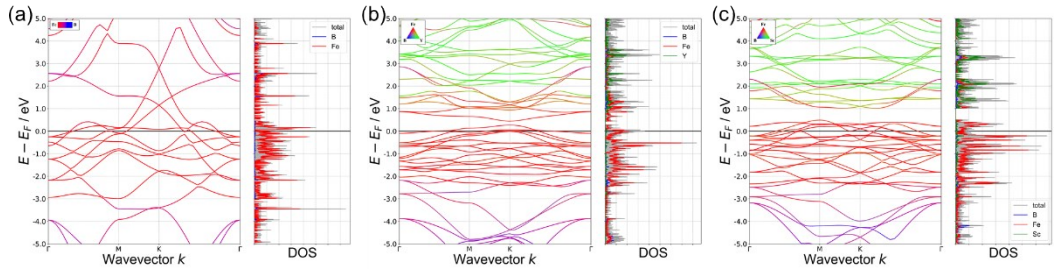

Figure S18. Calculated band structure and projected DOS for (a)Fe_2B_2, (b) $(Fe_{2/3}Sc_{1/3})_2B_2$, (c) $(Fe_{2/3}Y_{1/3})_2B_2$.

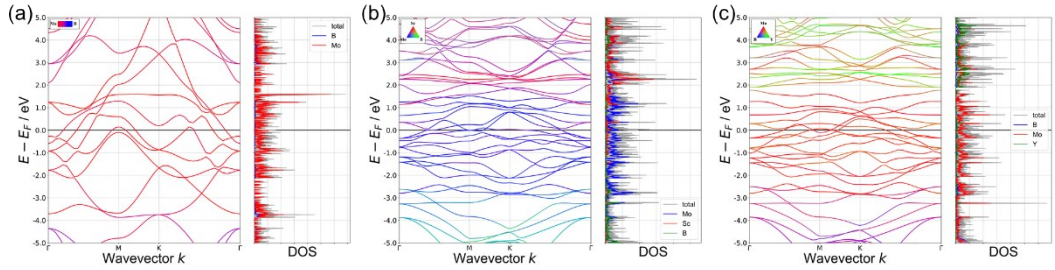

Figure S19. Calculated band structure and projected DOS for (a)Mo_2B_2, (b) $(Mo_{2/3}Sc_{1/3})_2B_2$, (c) $(Mo_{2/3}Y_{1/3})_2B_2$.

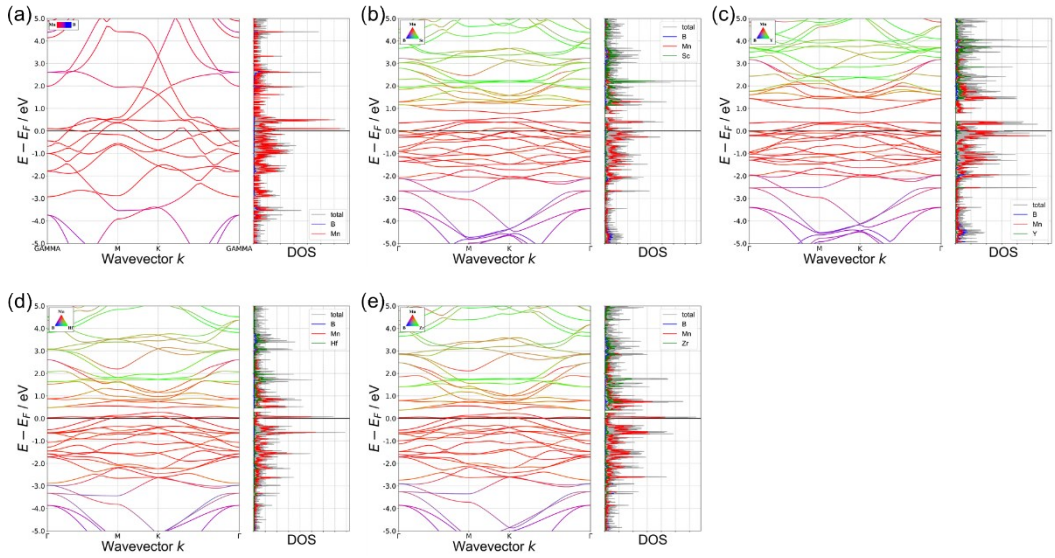

Figure S20. Calculated band structure and projected DOS for (a)Mn_2B_2, (b) $(Mn_{2/3}Sc_{1/3})_2B_2$, (c) $(Mn_{2/3}Y_{1/3})_2B_2$, (d) $(Mn_{2/3}Hf_{1/3})_2B_2$, (e) $(Mn_{2/3}Zr_{1/3})_2B_2$.

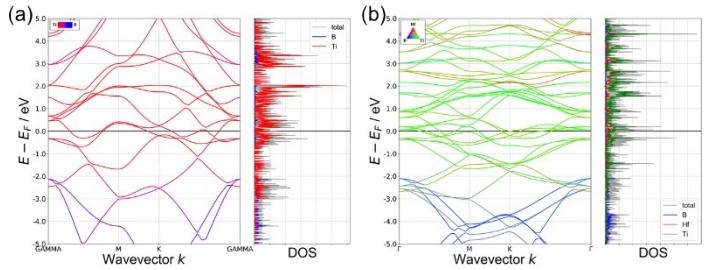

Figure S21. Calculated band structure and projected DOS for (a)Ti_2B_2, (b) $(Ti_{2/3}Hf_{1/3})_2B_2$.

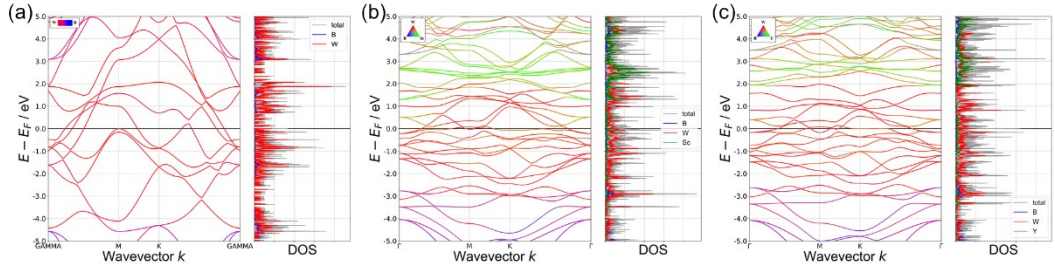

Figure S22. Calculated band structure and projected DOS for (a)W_2B_2, (b) $(W_{2/3}Sc_{1/3})_2B_2$, (c) $(W_{2/3}Y_{1/3})_2B_2$.

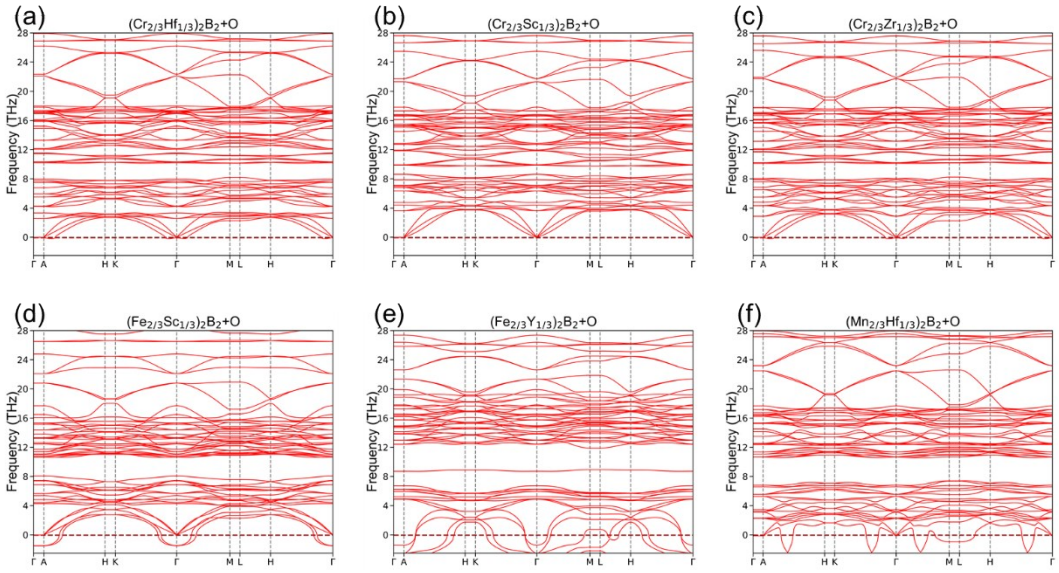

Figure S23. Phonon dispersion calculation for (a) $(Cr_{2/3}Hf_{1/3})_2B_2O_2$, (b) $(Cr_{2/3}Sc_{1/3})_2B_2O_2$, (c) $(Cr_{2/3}Zr_{1/3})_2B_2O_2$, (d) $(Fe_{2/3}Sc_{1/3})_2B_2O_2$, (e) $(Fe_{2/3}Y_{1/3})_2B_2O_2$, (f) $(Mn_{2/3}Hf_{1/3})_2B_2O_2$.

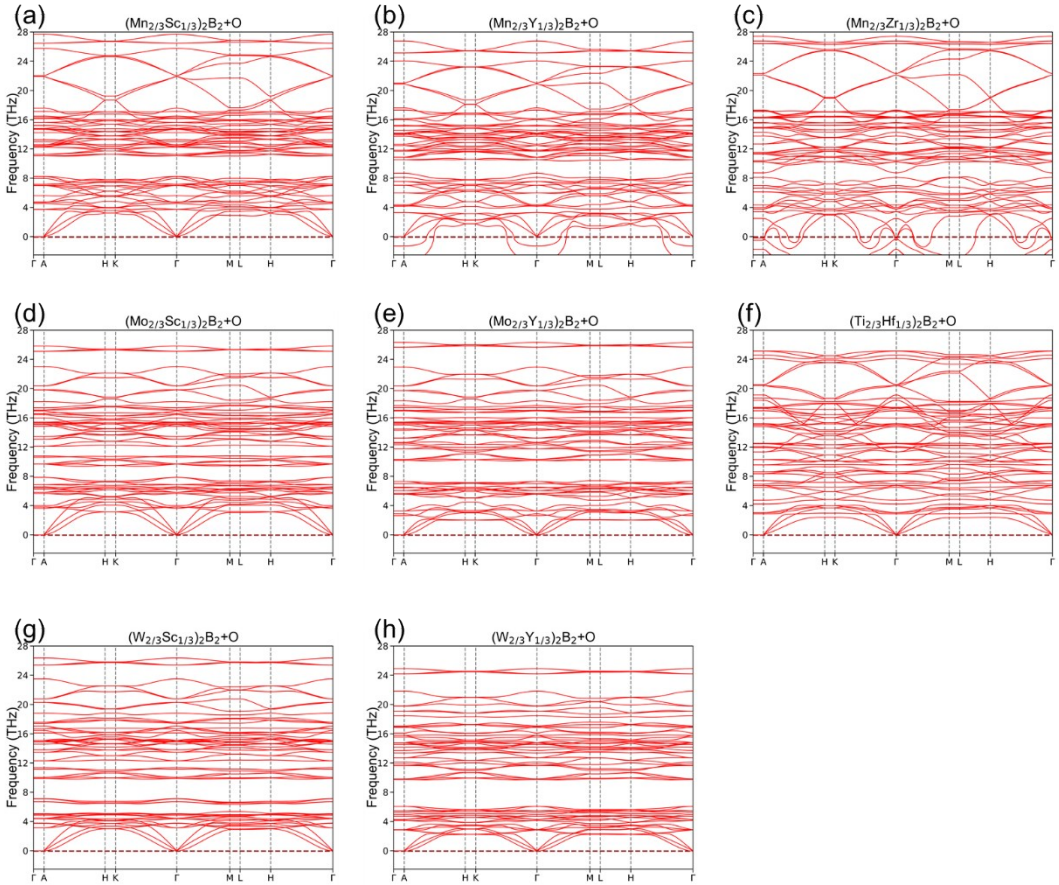

Figure S24. Phonon dispersion calculation for (a) $(Mn_{2/3}Sc_{1/3})_2B_2O_2$, (b) $(Mn_{2/3}Y_{1/3})_2B_2O_2$, (c) $(Mn_{2/3}Zr_{1/3})_2B_2O_2$, (d) $(Mo_{2/3}Sc_{1/3})_2B_2O_2$, (e) $(Mo_{2/3}Y_{1/3})_2B_2O_2$, (f) $(Ti_{2/3}Hf_{1/3})_2B_2O_2$, (g) $(W_{2/3}Sc_{1/3})_2B_2O_2$, (h) $(W_{2/3}Y_{1/3})_2B_2O_2$.

Supporting Tables

Table S1. Symmetry information and identified equilibrium simplex for $(M'_{2/3}M''_{1/3})_2AB_2$ composition.

A	M'	M''	Symmetry	Competing Phase
Al	W	Y	$R\bar{3}m$ (166)	AlBW, Al_5W, BW_2, YB_2
Al	Fe	Y	$P\bar{6}2c$ (190)	$Al(FeB)_2$, YB_2, Y_2Al, YAl_2
Al	Fe	Sc	$P\bar{6}2m$ (189)	$Al(FeB)_2$, ScB_2, ScAl
Al	Mn	Sc	$C2$ (5)	Mn_2AlB_2, ScB_2, ScAl
Al	Mn	Y	$P\bar{6}2c$ (190)	Mn_2AlB_2, YB_2 Y_2Al, YAl_2
Al	Mn	Zr	$R\bar{3}m$ (166)	Mn_2AlB_2, ZrB_2, Zr_4Al_3, Zr_2Al_3
Al	Mn	Hf	$R\bar{3}m$ (166)	Mn_2AlB_2, HfB_2, $HfAl_2$, Hf_4Al_3
Al	Mo	Y	$R\bar{3}m$ (166)	BMo, AlBMo, YB_2 YAl_2
Al	W	Sc	$R\bar{3}m$ (166)	AlBW, Al_5W, BW_2, ScB_2
Al	Mo	Sc	$R\bar{3}m$ (166)	BMo, $AlMo_3$, Al_8Mo_3, ScB_2
Al	Cr	Sc	$R\bar{3}m$ (166)	CrB, ScB_2, $ScAl_3$
Al	Ti	Hf	$P\bar{6}2m$ (189)	TiB_2, Ti_3Al, $HfAl_2$, Hf_4Al_3
Al	Mn	Nb	$R\bar{3}m$ (166)	Mn_2AlB_2, $NbAl_3$, Nb_5B_6
Al	Cr	Zr	$R\bar{3}m$ (166)	CrB, ZrB_2, $ZrAl_3$
Al	Cr	Hf	$R\bar{3}m$ (166)	$Al(CrB)_2$, $AlCr_2$, HfB_2, $HfAl_3$
Ga	Ti	Zr	$P\bar{6}2m$ (189)	TiB_2, Ti3B_4, Zr_2Al_3
Ga	Mn	Y	$P\bar{6}2c$ (190)	MnB_4, MnB, $MnGa_4$,YB_2,YGa
Ga	Mn	Sc	$P\bar{6}2c$ (190)	MnB_4, MnB, $MnGa_4$, ScB_2, ScGa
Ga	Mo	Y	$C2$ (5)	BMo, YB_4, YGa_2
Ga	Fe	Sc	$P\bar{6}2m$ (189)	FeB, ScB_2, Ga_3Fe
Ga	Sc	W	$C2$ (5)	ScB_2, BW_2, Sc_3Ga_5
Ga	Mn	Zr	$R\bar{3}m$ (166)	ZrB_2, Mn_2B, $MnGa_4$, MnB_4
Ga	Mn	Hf	$P\bar{6}2c$ (190)	$MnGa_4$, Mn_2B, HfB_2
Ga	Sc	Mo	$C2$ (5)	BMo, ScB_2, Sc_3G_5, $ScGa_3$
Ga	Mo	Sc	$R\bar{3}m$ (166)	BMo, ScB_2, $ScGa_3$
Ga	Mn	Nb	$R\bar{3}m$ (166)	NbB_2, MnB, Mn_2B, $MnGa_4$
Ga	Cr	Sc	$R\bar{3}m$ (166)	ScB_2, CrB, $ScGa_3$
Zn	Mo	Sc	$R\bar{3}m$ (166)	BMo, ScB_2, $ScZn_3$
Zn	Mo	Y	$R\bar{3}m$ (166)	BMo, YZn_3, YB_2
Zn	Mn	Sc	$C2$ (5)	MnB, ScB_2, $ScZn_3$
Zn	Ti	Hf	$P\bar{6}2m$ (189)	$HfZn_2$, TiB_2, Hf_2Zn, Ti_3B_4
Zn	Fe	Sc	$P\bar{6}2m$ (189)	ScB_2, $ScZn_3$, FeB
Zn	W	Sc	$R\bar{3}m$ (166)	BW_2, $ScZn_{12}$, ScB_2 ,BW
Zn	W	Y	$R\bar{3}m$ (166)	YZn_3, YB_2, BW
Si	Mn	Sc	$R\bar{3}m$ (166)	ScB_2, Mn_4Si_7, MnB
Si	Mo	Y	$R\bar{3}m$ (166)	YB_4, Bmo, YSi, Si_2Mo,
Si	Cr	Sc	$R\bar{3}m$ (166)	ScB_2, $CrSi_2$, CrB,
Si	V	Sc	$R\bar{3}m$ (166)	ScSi, ScB_2, VSi_2 V_2B3,
Si	Mn	Y	$P\bar{6}2c$ (190)	MnB, Mn_5Si_7, YB_4, YSi,
In	Sc	Mo	$C2$ (5)	$ScIn_2$, BMo, ScIn, ScB_2

Table S2. ICOHP, Force Constant and Bader Charge in Mo_2AlB_2, $(Mo_{2/3}Sc_{1/3})_2AlB_2$ and $(Mo_{2/3}Y_{1/3})_2AlB_2$.

		Mo_2AlB_2	$(Mo_{2/3}Sc_{1/3})_2AlB_2$	$(Mo_{2/3}Y_{1/3})_2AlB_2$
-ICOHP (eV/bond)	A-A	1.20	2.60	2.40
	B-B	5.75	5.54	5.38
	M-A	1.76	1.67(Mo)	1.38(Mo)
			0.64(Sc)	1.00(Y)
	M-B	1.76	1.99(Mo)	1.97(Mo)
			0.91(Sc)	1.29(Y)
Force Constant (eV/Å^2)	A-A	0.44	4.35	3.86
	B-B	6.76	7.10	6.64
	M-A	2.39	1.91(Mo)	1.79(Mo)
			1.64(Sc)	1.71(Y)
	M-B	3.92	5.01(Mo)	5.47(Mo)
			2.37(Sc)	2.41(Y)
Bader Charge (*e*)	A	2.34 (-0.66)	3.02 (0.02)	3.10 (0.10)
	B	3.50 (0.50)	3.59 (0.59)	3.57 (0.57)
	M	13.83 (-0.17)	13.90(Mo) (-0.16)	13.81(Mo) (-0.19)
			9.53(Sc) (-1.48)	9.50(Y) (-1.50)

Table S3. The absolute values of the separation energies of each quaternary *h*-MAB phases.

	M/B (J/m^2)	M/A (J/m^2)
$(Fe_{2/3}Y_{1/3})_2AlB_2$	6.79	2.15
$(Fe_{2/3}Sc_{1/3})_2AlB_2$	5.69	2.15
$(Cr_{2/3}Zr_{1/3})_2AlB_2$	7.07	3.16
$(Cr_{2/3}Hf_{1/3})_2AlB_2$	7.12	3.25
$(W_{2/3}Sc_{1/3})_2AlB_2$	6.42	2.96
$(Mn_{2/3}Y_{1/3})_2AlB_2$	7.76	3.60
$(Cr_{2/3}Sc_{1/3})_2AlB_2$	7.71	3.59
$(Mn_{2/3}Sc_{1/3})_2AlB_2$	7.65	3.61
$(Mo_{2/3}Y_{1/3})_2AlB_2$	7.18	3.42
$(Mn_{2/3}Hf_{1/3})_2AlB_2$	7.16	3.42
$(W_{2/3}Y_{1/3})_2AlB_2$	6.91	3.33
$(Ti_{2/3}Hf_{1/3})_2AlB_2$	6.92	3.39
$(Mo_{2/3}Sc_{1/3})_2AlB_2$	7.07	3.52
$(Mn_{2/3}Zr_{1/3})_2AlB_2$	7.71	3.87
$(Mn_{2/3}Nb_{1/3})_2AlB_2$	7.74	4.67